Geophysical Research Letters

RESEARCH LETTER
10.1029/2020GL088964

Key Points:
- The first laboratory "icequakes" were generated and slip stability was predicted well by rate-and-state friction
- Laboratory icequake attributes such as peak slip velocity, stress drop and healing agree well with other laboratory and field observations
- The laboratory icequake events suggest that debris-bed contacts dominate the sudden slip mechanics

Supporting Information:
- Supporting Information S1

Correspondence to:
L. K. Zoet,
lzoet@wisc.edu

Citation:
Zoet, L. K., Ikari, M. J., Alley, R. B., Marone, C., Anandakrishnan, S., Carpenter, B. M., et al. (2020). Application of constitutive friction laws to glacier seismicity. *Geophysical Research Letters*, *47*, e2020GL088964. https://doi.org/10.1029/2020GL088964

Received 21 MAY 2020
Accepted 12 OCT 2020
Accepted article online 19 OCT 2020

Application of Constitutive Friction Laws to Glacier Seismicity

L. K. Zoet[1], M. J. Ikari[2], R. B. Alley[3], C. Marone[3], S. Anandakrishnan[3], B. M. Carpenter[4], and M. M. Scuderi[5]

[1]Department of Geoscience, University of Wisconsin-Madison, Madison, WI, USA, [2]MARUM Center for Marine Environmental Sciences, and Faculty of Geosciences, University of Bremen, Bremen, Germany, [3]Department of Geosciences, and Earth and Environmental Systems Institute, Pennsylvania State University, University Park, PA, USA, [4]School of Geosciences, University of Oklahoma, Norman, OK, USA, [5]La Sapienza, Department of Earth Science, University of Rome, Rome, Italy

Abstract While analysis of glacial seismicity continues to be a widely used method for interpreting glacial processes, the underlying mechanics controlling glacial stick-slip seismicity remain speculative. Here, we report on laboratory shear experiments of debris-laden ice slid over a bedrock asperity under carefully controlled conditions. By modifying the elastic loading stiffness, we generated the first laboratory icequakes. Our work represents the first comprehensive lab observations of unstable ice-slip events and replicates several seismological field observations of glacier slip, such as slip velocity, stress drop, and the relationship between stress drop and recurrence interval. We also observe that stick-slips initiate above a critical driving velocity and that stress drop magnitude decreases with further increases in velocity, consistent with friction theory and rock-on-rock friction laboratory experiments. Our results demonstrate that glacier slip behavior can be accurately predicted by the constitutive rate-and-state friction laws that were developed for rock friction.

Plain Language Summary Glacier beds and tectonic faults may at first appear to be quite different, but they share important characteristics. In both cases, motion may be smooth (aseismic creep) or earthquake-producing "stick-slip." A powerful physical constitutive relationship called rate-and-state friction has been developed to understand earthquakes and smooth slip on tectonic faults. Laboratory experiments reported here simulate glacier-bed motion by sliding debris-bearing ice over a rock plate under conditions that are typical for glacier beds. They produce the first laboratory icequakes. Transitions between steady and stick-slip motions are generated by controlling shearing velocity and other conditions, as predicted by rate-and-state friction theory. Future studies can thus apply this physical framework to glacier slip, helping to understand ice motion and its potential to accelerate sea level rise in a warming world. Furthermore, because motion at the glacier bed is often much easier to study than tectonic faults, additional observations of glaciers may provide useful insights into earthquake behavior.

1. Introduction

Faster glacier flow into the ocean could accelerate sea-level rise. Motion of outlet glaciers is primarily controlled by slip at their bases (Cuffey & Paterson, 2010). The theoretical framework for estimating glacier slip has been developed largely in terms of stable, rate-strengthening slip (e.g., Schoof, 2005; Weertman, 1957; Zoet & Iverson, 2020), but widespread observations of basal seismicity show that unstable, rate-weakening (i.e., decreasing friction with increasing sliding speed) behavior also plays an important role in glacial motion. Unstable glacial slip may be akin to movements of a seismogenic fault, where periods of little or no motion are punctuated by periods of sudden acceleration and deceleration (Aster & Winberry, 2017). Basal-slip seismicity has been observed for many glacier morphologies and bed conditions, from Antarctic and Greenland ice streams (e.g., Blankenship et al., 1987; Bindschadler et al., 2003; Winberry et al., 2009, McBrearty et al., 2020) to alpine glaciers (e.g., Allstadt & Malone, 2014; Thelen et al., 2013) and from hard beds (more rigid than ice) to deformable beds (less rigid than ice), indicating that glaciers spanning the full spectrum of basal slip conditions can slip unstably under certain conditions. Even glaciers that appear to have stable surface motion may have much of their slip accommodated through the combination of many small-scale unstable slip events (McBrearty et al., 2020). A better understanding of unstable-slip

mechanics in glacial environments will provide a framework for interpreting the importance and implications of glacier seismicity. Furthermore, stick-slip behavior may accelerate glacier erosion under some conditions (Zoet, Alley, et al., 2013).

Glacier slip is typically characterized by noninertial stable slip, arising from the mechanisms of regelation and viscous creep (Kamb, 1970; Lliboutry, 1968; Nye, 1969; Schoof, 2005; Weertman, 1957; Zoet & Iverson, 2015, 2016) and sometimes through mean-stress-dependent (Coulomb) subglacial-till deformation (Blankenship et al., 1986; Zoet & Iverson, 2020). In these analyses, the slip/basal-deformation rate is estimated by assuming force balance between driving stress and basal resistive stress, which sets the slip speed. However, the presence of slip-generating seismicity is evidence of at least temporary force imbalances beneath glaciers (Aki & Richards, 2002). In some instances, the motion from basal seismicity can account for ~95% of the total glacier motion (Winberry et al., 2009; Zoet et al., 2012). On occasion, glaciers have switched between dominantly stable and unstable slip modes, potentially altering bulk flow of the glacier (Zoet et al., 2012). Constraining the mechanics that cause transition to unstable, stick-slip motion and icequakes would help assess the role of unstable slip in glacier motion.

Estimates of glacier-bed stress state from seismic observations of subglacial stick-slip behavior (e.g., Zoet, Alley, et al., 2013) have generally assumed that the unstable slip is similar to slip along tectonic faults (Aster & Winberry, 2017; Podolskiy & Walter, 2016). However, confirmation and extension of this assumption via laboratory experiments remain limited, with only a few studies of the physical processes that govern unstable slip at the ice-bed interface (e.g., Lipovsky et al., 2019; McCarthy et al., 2017; Zoet, Carpenter, et al., 2013). In particular, an open question is whether rate-and-state friction theory, which successfully describes the seismic cycle of tectonic faults (e.g., Marone, 1998; Rice et al., 2001), applies to glacier slip. Aspects of the ice-bed interface that vary from traditional rock-rock friction may render cryogenic slip events fundamentally different from tectonic slip events, and thus, use of rate-and-state friction may be inappropriate. For example, the rheological contrast across the glacier-bed fault (i.e., one side of the fault is ice or debris-bearing ice) is larger than for most tectonic settings, and the ice exhibits stick-slip behavior despite being a viscoelastic material at/near its pressure melting point.

To investigate the mechanics of unstable glacier slip, we conducted experiments in which debris-laden ice was sheared over a simulated bedrock asperity (Westerly Granite) in a biaxial shearing device. To explore a wide range of slip behaviors in a continuum parameter space, we modified the shear loading stiffness of the apparatus (Leeman et al., 2016). We compare the resulting laboratory "icequakes" with results of traditional rock slip experiments and field glacier seismicity, to better constrain the underlying physics controlling unstable glacier slip.

2. Materials and Methods

2.1. Sample Preparation

Our debris-laden ice was prepared to closely resemble natural glacier basal ice. Ice samples containing randomly distributed debris of amphibole schist with a bimodal grain-size distribution, as in Zoet, Carpenter, et al. (2013), were constructed using debris extracted from the basal ice of Engabreen, Norway, and in one experiment, a sample of actual debris basal ice extracted from Engabreen was used (see supporting information Table S1). The debris-laden ice samples were sheared against Westerly Granite, which was milled flat and polished with a 60 grit finish. The samples contained 16–28% debris by volume, matching the range of debris content in Engabreen basal ice (Zoet, Carpenter, et al., 2013). The debris-laden ice samples were 4.5 × 7.0 × 1.0 cm, and the Westerly Granite was 4.5 × 5.0 × 1.0 cm. Both ice and Westerly Granite were set in steel carriage assemblies and placed in direct contact with the loading rams (see Figure S1). During shear, a constant contact area of 22.5 cm^2 was maintained. A thermistor inserted at the slip interface monitored temperature during shear (see Figure S2).

2.2. Experimental Apparatus

We used a servo-controlled biaxial testing apparatus in a single-direct configuration (Faoro et al., 2009), with stiffness modified to test stability (i.e., the occurrence or absence of stick-slip) of ice sliding over an asperity (Figure S1). The shear loading stiffness of the apparatus is much higher than the sample stiffness to induce stable slip during friction experiments. To investigate unstable slip conditions, the shear loading stiffness

was modified through the insertion of a chrome silicone spring in series with the shear ram (Leeman et al., 2016). The insertion of the spring resulted in poor displacement resolution of the sample carriage from the displacement transducer mounted to the load point on the driving ram. To resolve fine details of sample slip, an additional displacement transducer was mounted directly on the ice sample carriage, allowing measurement of sample motion including sudden accelerations. All other experimental procedures and temperature controls were as reported in Zoet, Carpenter, et al. (2013).

2.3. Procedure

The debris-laden ice sample was placed under a constant normal stress of 500 kPa, and the shearing ram was driven at a constant velocity past the stationary Westerly Granite sample. The imposed normal stress was larger than some measured subglacial effective stresses in glaciers that exhibit stick-slip, but normalizing the experimental shear stress values as friction coefficients allows a direct comparison to field data, though other normal stress-dependent processes could exist. The normal stress on the frictional surface was maintained using a fast-acting hydraulic servo controller accurate within ±5 kPa. Meltwater was allowed to drain from the interface, so fluid pressure could be assumed near atmospheric and the effective stress nearly equaled the applied normal stress. The shearing piston (vertical orientation in Figure S1) was driven at constant velocity, while shear stress was measured by an inline load cell. Data were recorded with 24 bit accuracy at rates up to 10 kHz, capturing sudden accelerations associated with stress drops (i.e., sudden decrease in shear stress). The samples were housed in a climate-controlled sample chamber, with temperature held constant at -3 ± 1°C as indicated by the thermistor installed at the ice-bed interface (Figure S2). The shear duration for each experiment was <25 min, minimizing temperature variability.

The driving velocity was increased stepwise from 10 to 60 or 10 to 100 μm s^{-1} to investigate slip stability over a range of velocities spanning the rate-strengthening to rate-weakening transition identified by Zoet, Carpenter, et al. (2013) for these experimental conditions. These values (~300–3,000 m yr^{-1}) are typical of fast-moving glaciers. To allow unstable slip to occur, the stiffness of the apparatus $k = \left|\frac{\Delta F}{\Delta u}\right|$ where ΔF is the change in force (N) and Δu is the displacement (m) was reduced below a critical value k_c, as predicted by rate-and state friction theory (e.g., Gu et al., 1984; Rice & Ruina, 1983). The k_c was estimated from the shear interface's frictional properties at velocities that experienced rate weakening, measured in the stiffened apparatus configuration of Zoet, Carpenter, et al. (2013) to be ~3.8×10^5 N m^{-1} (see Text S1). According to friction theory, when $k < k_c$, a force imbalance nucleated at the interface can propagate along the interface and drive slip acceleration (e.g., Cook, 1981; Scholz, 1998). Our apparatus stiffness was lowered to 1.1×10^5 N m^{-1} by insertion of the spring for a total of seven experiments (Figure S3), to meet the criterion of $k < k_c$. The spring simulates the ability of ice in a natural glacier surrounding a slip patch to store and release elastic strain energy in seismic events.

3. Results

Stable slip was observed at a driving velocity of v = 10 μm s^{-1}, but stick-slip began to occur when the driving velocity was increased to v = 60 μm s^{-1}, with measurable stress drops, $\Delta\tau$ (Figure 1). As velocity increased further to v = 100 μm s^{-1}, $\Delta\tau$ decreased in magnitude, and interevent time decreased.

Individual stick-slips recorded at sampling rates of 10 kHz revealed a median peak slip velocity of ~70 ± 30 mm s^{-1} (Figure 2a), associated with a mean $\Delta\tau$ of 103 ± 37 kPa. We measured mean acceleration of 4 m s^{-2} (Figure 2b) and mean displacement of 1.5 mm per slip event over 24 individual stress drops. Peak slip velocity increased with $\Delta\tau$ by ~1 m s^{-1} MPa^{-1} (Figure 3a). The rupture area, A, and shear modulus, G, were constant in the experiments, so seismic moment, $M_0 = G \cdot A \cdot d$, varied only as a function of displacement, d. A comparison between $\Delta\tau$ and M_o yielded a linear relationship over the range of $\Delta\tau$ measured (Figure S4).

Similar to prior studies of rock-rock friction (e.g., Marone et al., 1995), we find that stress drop increases approximately linearly with the log of recurrence interval (Figure 3b). The rate of change in $\Delta\tau$ with logarithm of time R_i was 90 kPa per decade for the recurrence time span of 12–135 s (Figure 3b). A positive relationship between slip displacement and $\Delta\tau$ of 23 mm MPa^{-1} was also observed.

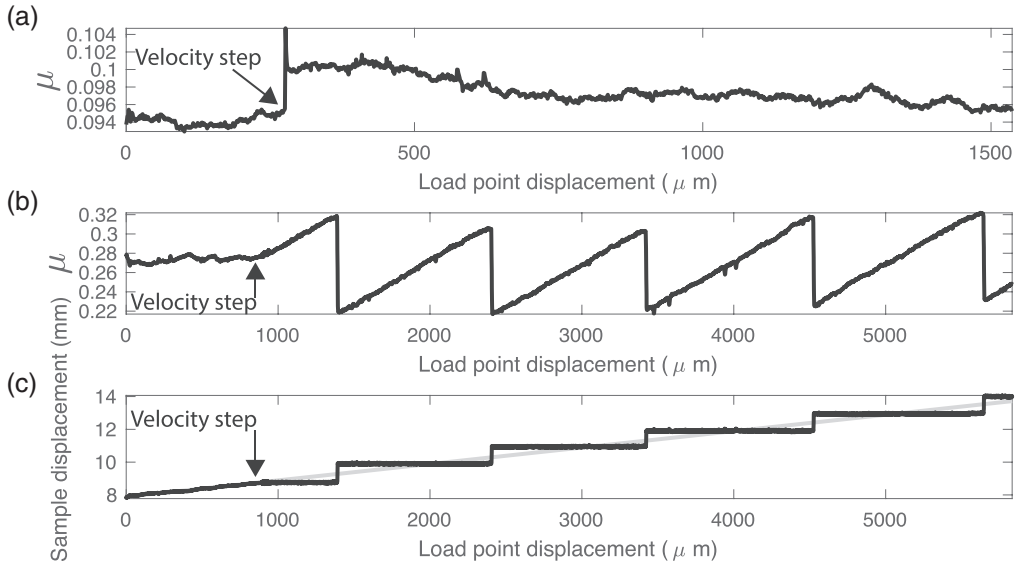

Figure 1. Friction data for a range of load point velocities. (a) Friction response to velocity steps from 10 to 60 μm s^{-1} under stiff conditions $k > k_c$. Note weakening trend but a lack of sudden stress drops. (b) Friction response for lower loading stiffness, with $k < k_c$. Note stick-slip motion and sudden stress drops. (c) Comparison of load point displacement (gray line) with displacement at the friction surface during stick-slip cycles (black line) shown in (b). There is a transition from stable displacement of the sample (diagonal section of black line) to stick-slips near load point displacement ~1,000 μm.

4. Discussion

Our experiments document unstable slip at the conditions predicted by rate-and-state friction laws. When the stiffness of the apparatus was below the critical value, k_c, a transition from stable to unstable slip occurred at the same velocities for which Zoet, Carpenter, et al. (2013) (Figure 1) measured a transition to rate weakening (i.e., a-b < 0, see Scholz, 1998, for further explanation of negative a-b values). Zoet, Carpenter, et al. (2013) showed that a sample containing 20–40% debris by volume at −3°C, such as those used here, exhibits a transition from velocity strengthening to velocity weakening frictional behavior at

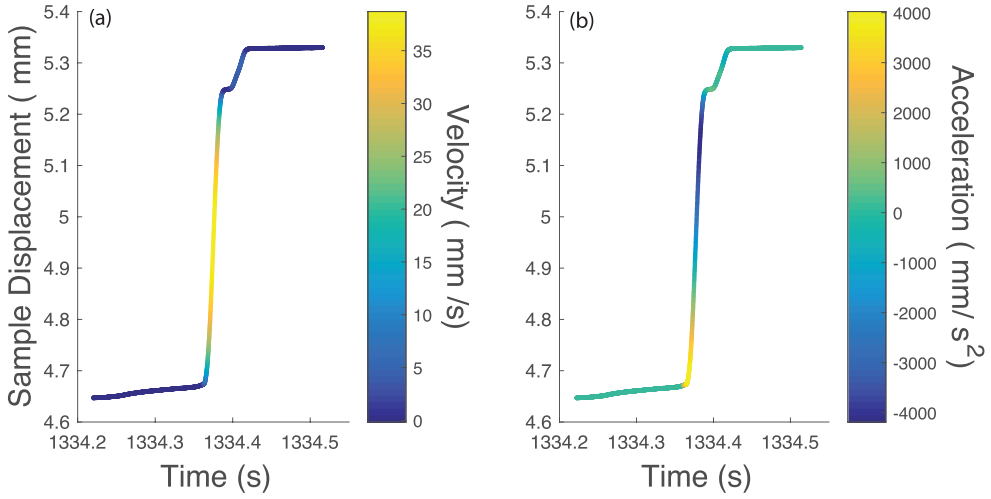

Figure 2. One representative stick-slip event. (a) The displacement and velocity were estimated from the displacement transducer mounted directly to the ice carriage. The color corresponds to the instantaneous velocity. (b) The second temporal derivative of the sample displacement was used to calculate the sample acceleration. The stick-slip starts with a strong acceleration and ends with a deceleration of similar magnitude.

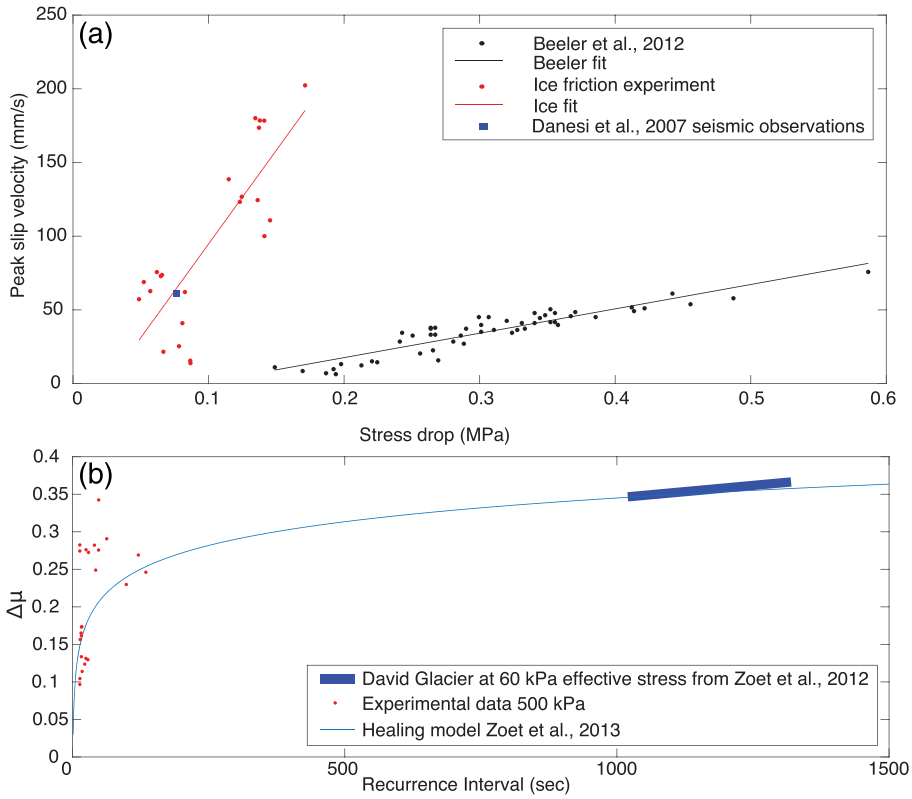

Figure 3. Comparison of field and laboratory data from experiments involving both rock and debris-bearing ice sliding over rock, for stress (or friction) drop associated with unstable slip events. (a) Comparison between stress drop and peak slip velocity. The black dots with the linear fit are from a rock-rock friction study by Beeler et al. (2012), who observed a linear relationship between peak slip velocity and stress drop. The red line is the trend between stress drop and peak slip velocity observed in this study, which also appears linear but with a larger slope. The blue square is the peak slip velocity and estimated stress drop of ~75 kPa observed at David Glacier using passive seismology (Danesi et al., 2007) (see Text S3 for an explanation of how stress drops were estimated). (b) Comparison of the friction drop (which is the stress drop normalized by effective normal stress) with recurrence interval time in seconds. Red dots show recurrence interval versus friction drop for the experimental icequakes. The solid blue line is the healing fit measured from Zoet, Carpenter, et al. (2013). The blue bar represents the range of friction drops versus recurrence intervals estimated by Zoet et al. (2012) from field seismic data for David Glacier, Antarctica (see Text S3). All data are expressed in terms of friction for comparison. For the experimental data, effective stress was 500 kPa, and for the field data corresponding to David glacier, an effective stress of 60 kPa was estimated.

velocities between 30 and 60 μm s^{-1}. Under these conditions, rate-and-state friction theory predicts that driving at velocities above these speeds in a less-stiff apparatus should produce stick-slips. The generation of stress drops when the velocity enters the rate-weakening velocity zone is in agreement with predictions for unstable slip via rate-and-state friction (Scholz, 1998) and supports conditional use of rate-and-state friction laws for describing glacier slip, as others have done (see Lipovsky & Dunham, 2016; Minchew & Meyer, 2020). The a, b, and D_c parameters measured for use in rate-and-state friction depend on in situ slip conditions and are therefore not simply material constants (Scholz, 1998).

Similarities between our laboratory icequake experiments and traditional rock-rock stick-slip experiments suggest similar underlying physical processes. We observe peak slip velocities that correlate positively with stress drop, approximately 1 m s^{-1} MPa^{-1}. In experiments conducted by Beeler et al. (2012) in which stick-slip was measured along a granite-granite contact, a positive relation between slip velocity and stress drop was also found, but with a slightly lower dependence of ~0.6 m s^{-1} MPa^{-1} (Figure 3a). Similarly, we observe a positive correlation between recurrence interval, R_i, and stress drop at 90 kPa per decade, similar to rock-rock slip experiments (e.g., Karner & Marone, 2000). In general, we observe correlations like those in rock mechanics experiments, although the trends are often slightly larger for ice-rock slip,

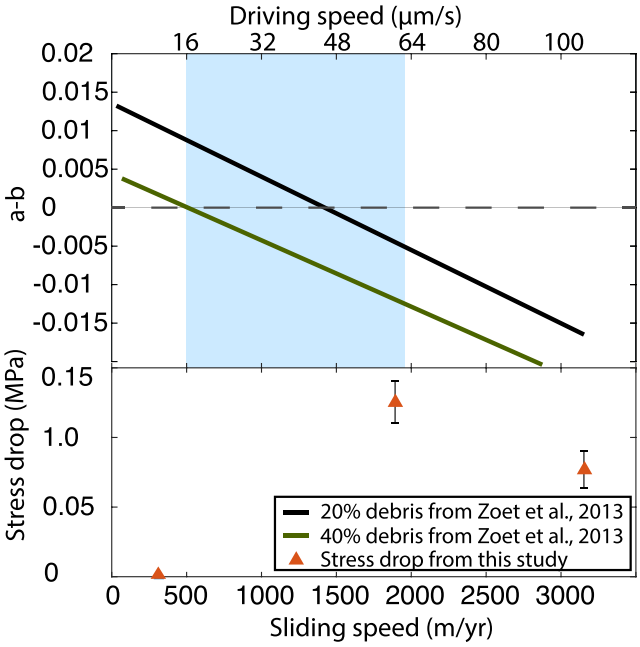

Figure 4. Dependence of stress drop and rate-and-state friction parameter a-b on sliding speed. The orange triangles represent the mean stress drop associated with a given sliding speed in the experiments. At all velocities where rate weakening was found to occur, the system was subcritically stiffened $k < k_c$. At 10 μm s^{-1}, only stable slip was observed, and so no associated stress drops were found (i.e., $\Delta\tau = 0$). At the sliding speed of 60 μm s^{-1}, the largest $\Delta\tau$ occurred, with smaller-magnitude $\Delta\tau$ at the highest sliding speed of 100 μm s^{-1}. Longer recurrence interval, R_i, occurred at slower sliding speeds that provided more time for healing, leading to greater stress drops. The solid lines represent a fit to the a-b results in Zoet, Carpenter, et al. (2013) for two different debris concentrations that bound the debris concentration used in this study. For 20% debris, a transition from velocity strengthening (a-$b > 0$) to velocity weakening (a-$b < 0$) was found at ~50 μm s^{-1}, while at a higher debris load, the transition was at ~18 μm s^{-1}. The sliding speed at which the Zoet, Carpenter, et al. (2013) data show a transition from velocity strengthening to velocity weakening approximately matches the speed at which the new data here show onset of $\Delta\tau$. Finally, the blue box represents a range of glacier slip speeds that commonly are observed to produce seismicity. The 500 m yr^{-1} lower bound is approximately the speed of David Glacier. Note, though, that some subglacial seismicity is observed outside this range (e.g., Anandakrishnan & Alley, 1997).

likely owing to the different mechanical properties of debris-laden ice versus intact rock. This is in part because stress drops in the ice-rock experiments are smaller than in rock-rock experiments. Possible explanation for this trend is a dependence of the stress drop on normal stress (Beeler et al., 2012) or that because the shear modulus of ice is ~10% of intact rock that may result in a proportional reduction in stress drop (Aki & Richards, 2002).

The laboratory icequakes also show characteristics similar to those estimated from field seismic observations for subglacial stick-slip icequakes. The maximum slip velocities observed in our experiments (~70 mm s^{-1}) closely resemble peak slip velocity estimated from seismic data by Danesi et al. (2007) of ~60 mm s^{-1} for subglacial icequakes at David Glacier in Antarctica (Figure 3b). Furthermore, the mean displacement of our laboratory slips of ~1.5 mm is consistent with estimated mean subglacial seismic slips of ~1.9 mm for a wide range of glacier settings (Figure 2) (Zoet, Alley, et al., 2013) even though our fault was unbounded and much smaller than the rupture area of real glaciers (Helmstetter et al., 2015; Roeoesli et al., 2016; Zoet et al., 2012).

Several studies have suggested that the underlying microphysical mechanisms of rate-and-state friction are related to healing along a fault interface, in part due to changing "real area of contact" from plastic deformation at grain-scale asperities via creep mechanisms (e.g., Baumberger & Caroli, 2006; Dieterich & Kilgore, 1994; Perfettini & Molinari, 2017). These processes result in a logarithmic healing curve for tectonic faults. Creep of ice is a well-established mechanism for ice deformation around larger asperities that characterize the glacier bed (Zoet & Iverson, 2016), but for debris-laden ice, the clast-bedrock contacts dominate sudden frictional slip (Hansen & Zoet, 2019; Thompson et al., 2020; Zoet, Carpenter, et al., 2013). In order to assess the relationship between healing at the ice-bed interface during times of no slip (stick) and the stress drop associated with the sudden slip, the logarithmic healing rate measured in Zoet, Carpenter, et al. (2013) for the same experimental conditions was applied (Figure 3b). The healing rate provides a reasonable fit to the experimental stress drop data but also approximates the stress drop for field seismic observations at David Glacier well (Figure 3b). Note that stress in Figure 3b has been normalized by effective stress to produce friction, μ, allowing for a direct comparison between the field and experimental data. The similarity in healing mechanisms manifested in a logarithmic healing rate active along both fault contacts and glacier ice-bed interface, albeit at different timescales, is a potential explanation for why constitutive rate-and-state friction laws are capable of predicting slip stability along the bed.

Successfully applying experimental results to natural phenomena requires realistic simulation of natural conditions. In our experiments, we in general replicated in situ temperature, stress, debris content, and driving velocity. In particular, natural driving rates are rarely achieved in rock friction experiments (see Ikari, 2019; Weeks, 1993) but were accomplished here, replicating an important natural boundary condition. For example, from satellite measurements, it is estimated that the seismically active region of David Glacier has a surface velocity of ~510 m yr^{-1} (16 μm s^{-1}) (Rignot et al., 2011) and most (~90%) of the surface velocity is likely the result of basal slip (see Text S2 for estimate of slip velocity). Our experimental data predict that frictional instability, manifested as stick-slip behavior, is possible at driving rates above 10 μm s^{-1} (or 315 m yr^{-1}) for realistic debris contents (Figure 4), which may explain why David Glacier is seismically active. It should be noted that these experiments are not intended to exactly simulate the basal conditions of David Glacier, as many of the independent parameters in the natural setting are

unknown. However, the events at David Glacier allow certain seismic attributes (e.g., stress drop and fault patch size) to be estimated, facilitating a first general comparison between laboratory and field measurements for icequakes.

These experiments have been conducted for a limited range of glaciological conditions (e.g., sliding speed, temperature, debris content, fault patch size, stress, etc.), so their usefulness is not in simulating all aspects of glacier slip but rather in demonstrating the applicability of the constitutive rate-and-state friction laws for subglacial slip in a general sense. Simply, if a rate-weakening response exists, for whatever reason (i.e., drained bed conditions, temperature, debris content, etc.), unstable slip and seismicity may be produced if other necessary conditions are met (e.g., a subcritically stiffened system and an interface capable of healing). Our experimental fault is much smaller than a detectable natural slip event and is unbounded on its sides. These boundary conditions likely render our experimental shear surfaces more akin to a small patch within a larger slipping fault rather than an isolated, very small slipping fault. Lipovsky et al. (2019) showed how the movement of a basal frozen fringe atop a till layer can approximate many of the same mechanics as debris-laden ice slipping over a hard bed, leading to rate-weakening slip. Furthermore, Zoet and Iverson (2018) showed how a deformable till bed can heal during periods between slip, which is the other requirement (in addition to rate weakening) for the occurrence of stick-slip. The potential similarities between processes active on hard and soft beds suggest that many of the mechanisms previously described for seismogenic glacier slip over hard beds may be applicable to soft beds.

5. Conclusions

In the new experiments and in preexisting data from field and laboratory discussed here, rate-and-state friction laws predict the slip stability of glaciers relatively well. The reasonably good fit between seismically derived estimates of slip and our laboratory estimates indicates that the constitutive rate-and-state friction laws may be appropriate for estimating glacier slip in certain circumstances (Lipovsky & Dunham, 2016; Thøgersen et al., 2019). Furthermore, the apparent similarity between tectonic faults and glacier slip may mean glaciers could be used as a suitable analog for tectonic slip in certain instances. Numerical modeling studies have shown a wide range of predictions for sea-level rise based on the use of various slip relationships (Ritz et al., 2015), and the results of this study at a minimum support the further development of glacier models that use rate-and-state friction to parameterize the basal slip.

Data Availability Statement

The data are available at the UW@MINDS repository (https://minds.wisconsin.edu/handle/1793/80316).

Acknowledgments

This research was funded by the Office of Polar Programs, U.S. National Science Foundation (NSF 0424589). Partial support was provided by the U.S. National Science Foundation through grants 0424589, 0538195, 0907178, 0944286, and 1738934 and the Sloan Program. We thank Fabian Walter and two anonymous reviewers whose comments improved the clarity of the manuscript. We are grateful for laboratory assistance from Lana Zoet and Peter Burkett.

References

Aki, K., & Richards, P. G. (2002). *Quantitative seismology*. Mill Valley, CA: University Science Books.

Allstadt, K., & Malone, S. D. (2014). Swarms of repeating stick-slip icequakes triggered by snow loading at Mount Rainier volcano. *Journal of Geophysical Research: Earth Surface*, *119*, 1180–1203. https://doi.org/10.1002/2014JF003086

Anandakrishnan, S., & Alley, R. B. (1997). Stagnation of ice stream C, West Antarctica by water piracy. *Geophysical Research Letters*, *24*(3), 265–268. https://doi.org/10.1029/96GL04016

Aster, R. C., & Winberry, J. P. (2017). Glacial seismology. *Reports on Progress in Physics*, *80*, 126801. https://doi.org/10.1088/1361-6633/aa8473

Baumberger, T., & Caroli, C. (2006). Solid friction from stick–slip down to pinning and aging. *Advances in Physics*, *55*(3–4), 279–348. https://doi.org/10.1080/00018730600732186

Beeler, N., Kilgore, B., McGarr, A., Fletcher, J., Evans, J., & Baker, S. R. (2012). Observed source parameters for dynamic rupture with non-uniform initial stress and relatively high fracture energy. *Journal of Structural Geology*, *38*, 77–89. https://doi.org/10.1016/j.jsg.2011.11.013

Bindschadler, R. A., King, M. A., Alley, R. B., Anandakrishnan, S., & Padman, L. (2003). Tidally controlled stick-slip discharge of a West Antarctic ice. *Science*, *301*(5636), 1087–1089. https://doi.org/10.1126/science.1087231

Blankenship, D. D., Anandakrishnan, S., Kempf, J. L., & Bentley, C. R. (1987). Microearthquakes under and alongside ice stream B, Antarctica. Detected by a new passive seismic array. *Annals of Glaciology*, *9*, 30–34. https://doi.org/10.3189/S0260305500200712

Blankenship, D. D., Bentley, C. R., Rooney, S. T., & Alley, R. B. (1986). Seismic measurements reveal a saturated porous layer beneath an active Antarctic ice stream. *Nature*, *322*(6074), 54–57. https://doi.org/10.1038/322054a0

Cook, N. G. (1981). *Stiff testing machines, stick slip sliding, and the stability of rock deformation*, *Geophysical Monograph Series* (Vol. 24, pp. 93–102). Washington, DC: American Geophysical Union.

Cuffey, K. M., & Paterson, W. S. B. (2010). *The physics of glaciers*. Amsterdam: Academic Press.

Danesi, S., Bannister, S., & Morelli, A. (2007). Repeating earthquakes from rupture of an asperity under an Antarctic outlet glacier. *Earth and Planetary Science Letters*, *253*(1–2), 151–158. https://doi.org/10.1016/j.epsl.2006.10.023

Dieterich, J. H., & Kilgore, B. D. (1994). Direct observation of frictional contacts: New insights for state-dependent properties. *Pure and Applied Geophysics*, *143*(1–3), 283–302. https://doi.org/10.1007/BF00874332

Faoro, I., Niemeijer, A., Marone, C., & Elsworth, D. (2009). Influence of shear and deviatoric stress on the evolution of permeability in fractured rock. *Journal of Geophysical Research*, *114*, B01201. https://doi.org/10.1029/2007JB005372

Gu, J. C., Rice, J. R., Ruina, A. L., & Simon, T. T. (1984). Slip motion and stability of a single degree of freedom elastic system with rate and state dependent friction. *Journal of the Mechanics and Physics of Solids*, *32*(3), 167–196. https://doi.org/10.1016/0022-5096(84)90007-3

Hansen, D. D., & Zoet, L. K. (2019). Experimental constraints on subglacial rock friction. *Annals of Glaciology*, *60*(80), 37–48. https://doi.org/10.1017/aog.2019.47

Helmstetter, A., Nicolas, B., Comon, P., & Gay, M. (2015). Basal icequakes recorded beneath an Alpine glacier (Glacier d'Argentière, Mont Blanc, France): Evidence for stick-slip motion? *Journal of Geophysical Research: Earth Surface*, *120*, 379–401. https://doi.org/10.1002/2014JF003288

Ikari, M. J. (2019). Laboratory slow slip events in natural geological materials. *Geophysical Journal International*, *218*(1), 354–387. https://doi.org/10.1093/gji/ggz143

Kamb, B. (1970). Sliding motion of glaciers: Theory and observation. *Reviews of Geophysics*, *8*(4), 673–728. https://doi.org/10.1029/RG008i004p00673

Karner, S. L., & Marone, C. (2000). *Effects of loading rate and normal stress on stress drop and stick-slip recurrence interval*, *Geophysical Monograph* (Vol. 120, pp. 187–198). Oxford, EN: American Geophysical Union.

Leeman, J. R., Saffer, D. M., Scuderi, M. M., & Marone, C. (2016). Laboratory observations of slow earthquakes and the spectrum of tectonic fault slip modes. *Nature Communications*, *7*, 11104. https://doi.org/10.1038/ncomms11104

Lipovsky, B. P., & Dunham, E. M. (2016). Tremor during ice-stream stick slip. *The Cryosphere*, *10*(1), 385–399. https://doi.org/10.5194/tc-10-385-2016

Lipovsky, B. P., Meyer, C. R., Zoet, L. K., McCarthy, C., Hansen, D. D., Rempel, A. W., & Gimbert, F. (2019). Glacier sliding, seismicity and sediment entrainment. *Annals of Glaciology*, *60*(79), 182–192. https://doi.org/10.1017/aog.2019.24

Lliboutry, L. (1968). General theory of subglacial cavitation and sliding of temperate glaciers. *Journal of Glaciology*, *7*(49), 21–58. https://doi.org/10.1017/S0022143000020396

Marone, C. (1998). Laboratory-derived friction laws and their application to seismic faulting. *Annual Review of Earth and Planetary Sciences*, *26*(1), 643–696. https://doi.org/10.1146/annurev.earth.26.1.643

Marone, C., Vidale, J. E., & Ellsworth, W. L. (1995). Fault healing inferred from time dependent variations in source properties of repeating earthquakes. *Geophysical Research Letters*, *22*(22), 3095–3098. https://doi.org/10.1029/95GL03076

McBrearty, I. W., Zoet, L. K., & Anandakrishnan, S. (2020). Basal seismicity of the Northeast Greenland Ice Stream. *Journal of Glaciology*, *66*(257), 430–446. https://doi.org/10.1017/jog.2020.17

McCarthy, C., Savage, H., & Nettles, M. (2017). Temperature dependence of ice-on-rock friction at realistic glacier conditions. *Philosophical Transactions of the Royal Society A: Mathematical, Physical and Engineering Sciences*, *375*, 20150348. https://doi.org/10.1098/rsta.2015.0348

Minchew, B. M., & Meyer, C. R. (2020). Dilation of subglacial sediment governs incipient surge motion in glaciers with deformable beds. *Proceedings of the Royal Society A*, *476*, 20200033. https://doi.org/10.1098/rspa.2020.0033

Nye, J. F. (1969). A calculation on the sliding of ice over a wavy surface using a Newtonian viscous approximation. *Proceedings of the Royal Society of London. A. Mathematical and Physical Sciences*, *311*(1506), 445–467. https://doi.org/10.1098/rspa.1969.0127

Perfettini, H., & Molinari, A. (2017). A micromechanical model of rate and state friction: 1. Static and dynamic sliding. *Journal of Geophysical Research: Solid Earth*, *122*, 2590–2637. https://doi.org/10.1002/2016JB013302

Podolskiy, E. A., & Walter, F. (2016). Cryoseismology. *Reviews of Geophysics*, *54*, 708–758. https://doi.org/10.1002/2016RG000526

Rice, J. R., Lapusta, N., & Ranjith, K. (2001). Rate and state dependent friction and the stability of sliding between elastically deformable solids. *Journal of the Mechanics and Physics of Solids*, *49*(9), 1865–1898. https://doi.org/10.1016/S0022-5096(01)00042-4

Rice, J. R., & Ruina, A. L. (1983). Stability of steady frictional slipping. *Journal of Applied Mechanics*, *50*(2), 343–349. https://doi.org/10.1115/1.3167042

Rignot, E., Mouginot, J., & Scheuchl, B. (2011). Ice flow of the Antarctic ice sheet. *Science*, *333*(6048), 1427–1430. https://doi.org/10.1126/science.1208336

Ritz, C., Edwards, T. L., Durand, G., Payne, A. J., Peyaud, V., & Hindmarsh, R. C. (2015). Potential sea-level rise from Antarctic ice-sheet instability constrained by observations. *Nature*, *528*(7580), 115–118. https://doi.org/10.1038/nature16147

Roeoesli, C., Helmstetter, A., Walter, F., & Kissling, E. (2016). Meltwater influences on deep stick-slip icequakes near the base of the Greenland Ice Sheet. *Journal of Geophysical Research: Earth Surface*, *121*, 223–240. https://doi.org/10.1002/2015JF003601

Scholz, C. H. (1998). Earthquakes and friction laws. *Nature*, *391*(6662), 37–42. https://doi.org/10.1038/34097

Schoof, C. (2005). The effect of cavitation on glacier sliding. *Proceedings of the Royal Society A: Mathematical, Physical and Engineering Sciences*, *461*(2055), 609–627. https://doi.org/10.1098/rspa.2004.1350

Thelen, W. A., Allstadt, K., De Angelis, S., Malone, S. D., Moran, S. C., & Vidale, J. (2013). Shallow repeating seismic events under an alpine glacier at Mount Rainier, Washington, USA. *Journal of Glaciology*, *59*(214), 345–356. https://doi.org/10.3189/2013JoG12J111

Thøgersen, K., Gilbert, A., Schuler, T. V., & Malthe-Sørenssen, A. (2019). Rate-and-state friction explains glacier surge propagation. *Nature Communications*, *10*, 2823. https://doi.org/10.1038/s41467-019-10506-4

Thompson, A. C., Iverson, N. R., & Zoet, L. K. (2020). Controls on subglacial rock friction: Experiments with debris in temperate ice. *Journal of Geophysical Research: Earth Surface*, *125*, e2020JF005718. https://doi.org/10.1029/2020JF005718

Weeks, J. D. (1993). Constitutive laws for high-velocity frictional sliding and their influence on stress drop during unstable slip. *Journal of Geophysical Research*, *98*(B10), 17,637–17,648. https://doi.org/10.1029/93JB00356

Weertman, J. (1957). On the sliding of glaciers. *Journal of Glaciology*, *3*(21), 33–38. https://doi.org/10.1017/S0022143000024709

Winberry, J. P., Anandakrishnan, S., Alley, R. B., Bindschadler, R. A., & King, M. A. (2009). Basal mechanics of ice streams: Insights from the stick-slip motion of Whillans Ice Stream, West Antarctica. *Journal of Geophysical Research*, *114*, F01016. https://doi.org/10.1029/2008JF001035

Zoet, L. K., Alley, R. B., Anandakrishnan, S., & Christianson, K. (2013). Accelerated subglacial erosion in response to stick-slip motion. *Geology*, *41*(2), 159–162. https://doi.org/10.1130/G33624.1

Zoet, L. K., Anandakrishnan, S., Alley, R. B., Nyblade, A. A., & Wiens, D. A. (2012). Motion of an Antarctic glacier by repeated tidally modulated earthquakes. *Nature Geoscience*, *5*(9), 623–626. https://doi.org/10.1038/ngeo1555

Zoet, L. K., Carpenter, B., Scuderi, M., Alley, R. B., Anandakrishnan, S., Marone, C., & Jackson, M. (2013). The effects of entrained debris on the basal sliding stability of a glacier. *Journal of Geophysical Research: Earth Surface*, *118*, 656–666. https://doi.org/10.1002/jgrf.20052

Zoet, L. K., & Iverson, N. R. (2015). Experimental determination of a double-valued drag relationship for glacier sliding. *Journal of Glaciology*, *61*(225), 1–7. https://doi.org/10.3189/2015JoG14J174

Zoet, L. K., & Iverson, N. R. (2016). Rate-weakening drag during glacier sliding. *Journal of Geophysical Research: Earth Surface*, *121*, 1206–1217. https://doi.org/10.1002/2016JF003909

Zoet, L. K., & Iverson, N. R. (2018). A healing mechanism for stick-slip of glaciers. *Geology*, *46*(9), 807–810. https://doi.org/10.1130/G45099.1

Zoet, L. K., & Iverson, N. R. (2020). A slip law for glaciers on deformable beds. *Science*, *368*(6486), 76–78. https://doi.org/10.1126/science.aaz1183

References From the Supporting Information

Dieterich, J. H. (1992). Earthquake nucleation on faults with rate-and state-dependent strength. *Tectonophysics*, *211*(1–4), 115–134. https://doi.org/10.1016/0040-1951(92)90055-B

Kanamori, H., & Anderson, D. L. (1975). Theoretical basis of some empirical relations in seismology. *Bulletin of the Seismological Society of America*, *65*(5), 1073–1095.

Morlighem, M., Rignot, E., Binder, T., Blankenship, D., Drews, R., Eagles, G., et al. (2020). Deep glacial troughs and stabilizing ridges unveiled beneath the margins of the Antarctic ice sheet. *Nature Geoscience*, *13*(2), 132–137. https://doi.org/10.1038/s41561-019-0510-8

Nye, J. F. (1952). The mechanics of glacier flow. *Journal of Glaciology*, *2*(12), 82–93. https://doi.org/10.1017/S0022143000033967

Geophysical Research Letters

Supporting Information for

Application of Constitutive Friction Laws to Glacier Seismicity

L.K Zoet[1], M.J. Ikari[2], R.B. Alley[3], C. Marone[3], S. Anandakrishnan[3], B.M. Carpenter[4], M.M. Scuderi[5]

[1] Department of Geoscience, University of Wisconsin-Madison, WI, 53704.

[2] MARUM Center for Marine Environmental Sciences, University of Bremen, Bremen, Germany D- 28359

[3] Department of Geosciences, and Earth and Environmental Systems Institute, Pennsylvania State University, University Park, PA, 16802.

[4] School of Geosciences, University of Oklahoma, Norman, OK 73019

[5] La Sapienza, Department of Earth Science, University of Rome, P.le Aldo Moro 5, Rome, Italy.

Contents of this file

Introduction

The supporting information includes an estimate of the experimental k_c, the basal velocity and seismic stress drop from David Glacier. It also contains additional figures of the experimental device and raw data. A table of the experimental parameters is also provided.

Supporting Text S1

To estimate the critical stiffness, k_c, we follow the method of Dieterich, 1992 (his equations 12 and 13) in which

$$k_c = \frac{(b-a)\eta\sigma}{D_c}, \qquad \text{(S1)}$$

where the values below were used to estimate k_c. k_c in the above expression produces units of [stress / length], and so to convert to the more traditional stiffness unit system of [force / length] the above expression was multiplied by the contact area, A. The k_c was calculated using the values in the table below. Note that k_c is calculated only for negative a-b values. For this project we have chosen the 30 to 60 μm s^{-1} velocity step from Zoet et al., (2013b), as that velocity step lies in the center of the relatively narrow velocity stepping range for this set of experiments.

Variable	Explanation	Value [units]	Source
b-a	Frictional weakening	0.01 [ ]	Zoet et al., (2013b) Fig 8b for 20% debris at 30 → 60 μm s^{-1} velocity step
D_c	Characteristic slip distance	30 [μm]	Zoet et al., (2013b)
σ	Normal stress	500 [kPa]	This study
η	Geometric factor	1 [ ]	Dieterich, (1992)
A	Area of the contact	0.00225 [m^2]	

Supporting Text S2

Using the equation below from Nye (1952), the basal slip velocity, u_b, for David Glacier can be estimated from the surface velocity:

$$u_b = u_s - \frac{2}{n+1}\frac{(\rho g \sin\alpha)^n}{B^n} H^{n+1} \qquad \text{(S2)}$$

where the values used to evaluate equation S2 are from the table below. It was found that basal slip accounted ~470 m/yr of the 510 m/yr (92%) surface velocity.

Variable	Explanation	Value [units]	Source
n	Glen exponent	3	Cuffey and Paterson (2010)
ρ	Ice density	910 [kg/m^3]	Cuffey and Paterson (2010)
α	Surface slope	1.1°	Zoet et al., (2012)
g	Gravitational constant	9.81 [m /s^2]	Cuffey and Paterson (2010)

B	Ice viscosity	1.418 x 10^8 [$Pa^{1/3}$ s]	Cuffey and Paterson (2010)
H	Ice thickness	1100 [m]	Morlighem et al., (2020)
u_s	Surface velocity	510 [m/yr]	Rignot et al., (2011)

Supporting Text S3

Stress drop, $\Delta\sigma$, for David Glacier was estimated from seismic moment, M_o, and fault radius, R, following the Kanamori and Anderson (1975) model:

$$\Delta\sigma = \frac{M_0}{a\,A^{3/2}}, \qquad \text{(S3)}$$

where A is the fault patch area and if a circular fault patch is assume A will equal the following:

$$A = \pi R^2. \qquad \text{(S4)}$$

Variable	Explanation	Value [units]	Source
M_o	Seismic moment	$3.8 \cdot 10^{11}$ [N m]	Danesi et al. (2007)
R	Radius	130 [m]	Danesi et al. (2007)
a	Geometric factor	0.41	Kanamori and Anderson (1975)
M_o	Seismic moment range	$3.1 - 5.2 \cdot 10^{11}$ [N m]	Zoet et al. (2012)
R	Radius range	$300 - 350$ [m]	Zoet et al. (2012)
a	Geometric factor	0.1	Zoet et al. (2012)

This analysis yields stress drops from Zoet et al. (2012) between 20-21 kPa while Danesi et al. (2007)'s events are ~75 kPa. If the geometric factor and fault radius from Zoet et al. (2012) are used to reevaluate Danesi et al. (2007)'s data, a stress drop of 19 kPa is estimated.

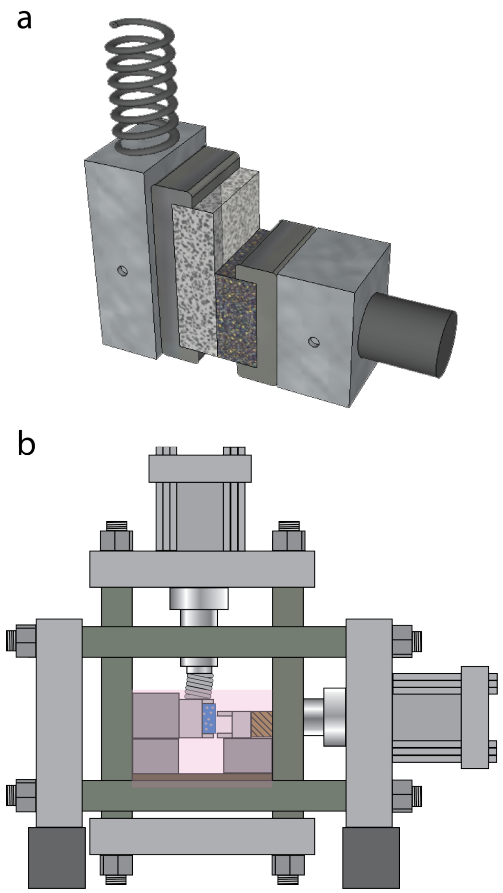

Figure S1: A schematic of the biaxial shearing device. **(a)** A schematic of the sample carriage assembly with the spring placement used to reduce the stiffness of the device. Debris laden ice is housed on the left side of the assembly while Westerly Granite is housed in the right. An additional displacement transducer was mounted directly to the debris laden ice carriage **(b)** The biaxial shear at large. The vertical ram provides the shear displacement while the horizontal ram provides the normal load. The pink shaded area was a temperature controlled insulated box that was regulated following the protocols outlined in Zoet et al., (2013b).

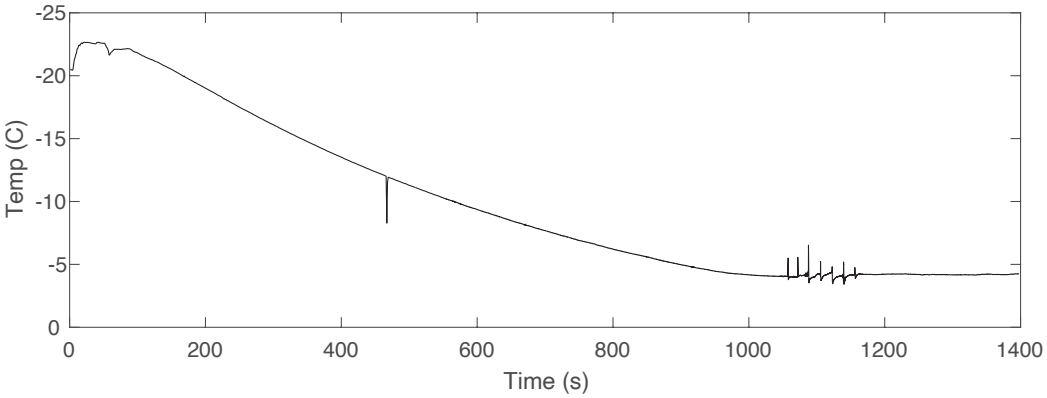

Figure S2: A temperature time series from experiment p3347. Initially the temperature was below the target temp of -3 ºC but was allowed to warm until approximately 1050 second mark when the temperature reached the target value and sliding was initiated. Prior to this time the sample was stationary. The mean temperature during slip for this experiment was -3.9 ºC.

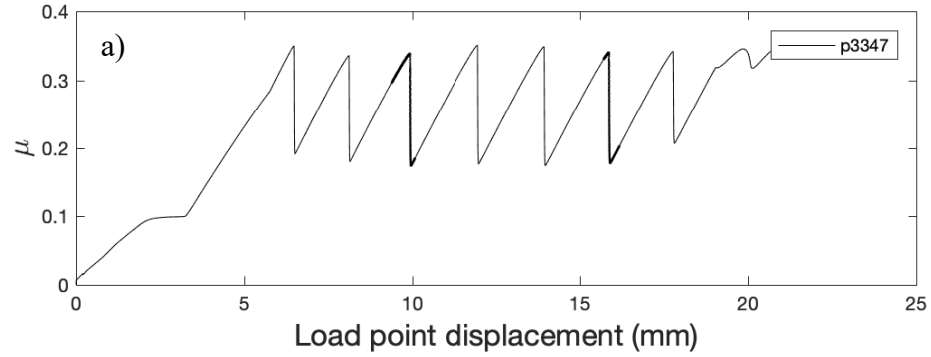
a)
p3347
μ
0.4
0.3
0.2
0.1
0
0
5
10
15
20
25
Load point displacement (mm)

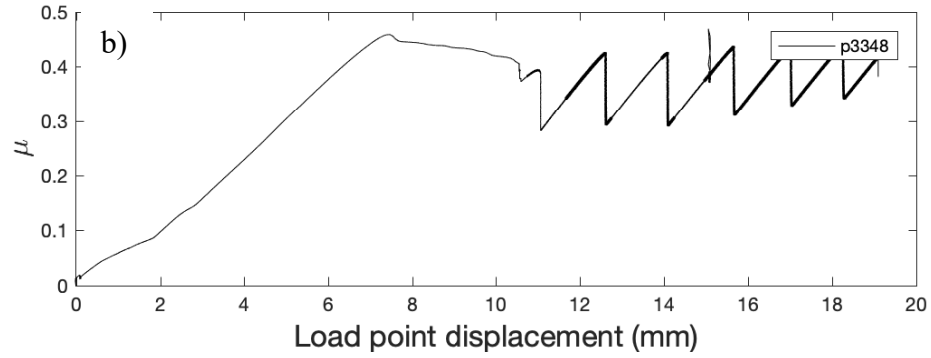
b)
p3348
μ
0.5
0.4
0.3
0.2
0.1
0
0
2
4
6
8
10
12
14
16
18
20
Load point displacement (mm)

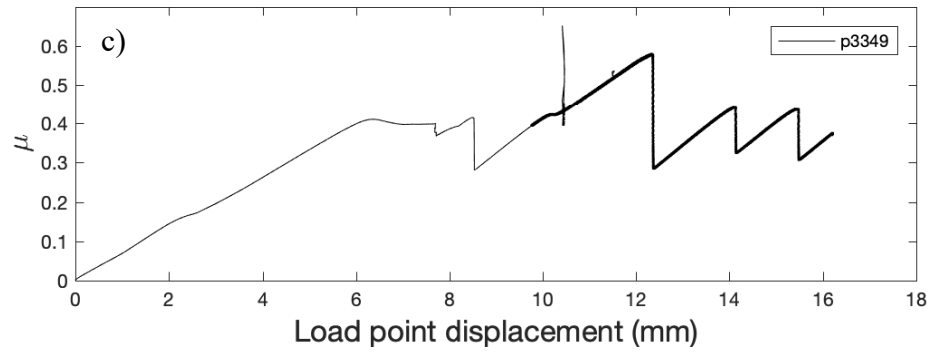
c)
p3349
μ
0.6
0.5
0.4
0.3
0.2
0.1
0
0
2
4
6
8
10
12
14
16
18
Load point displacement (mm)

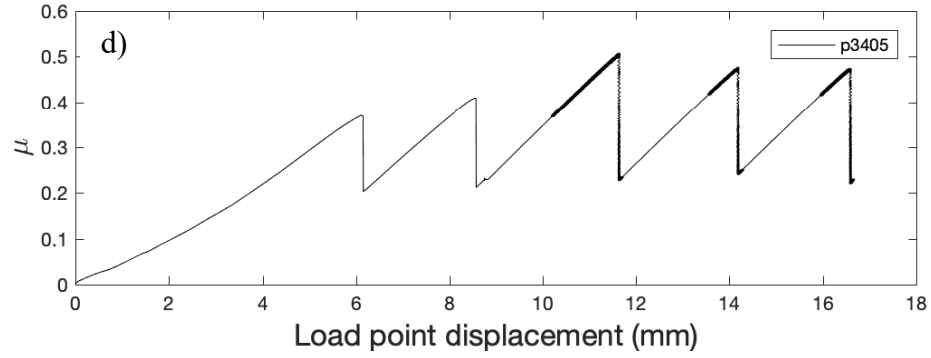
d)
p3405
μ
0.6
0.5
0.4
0.3
0.2
0.1
0
0
2
4
6
8
10
12
14
16
18
Load point displacement (mm)

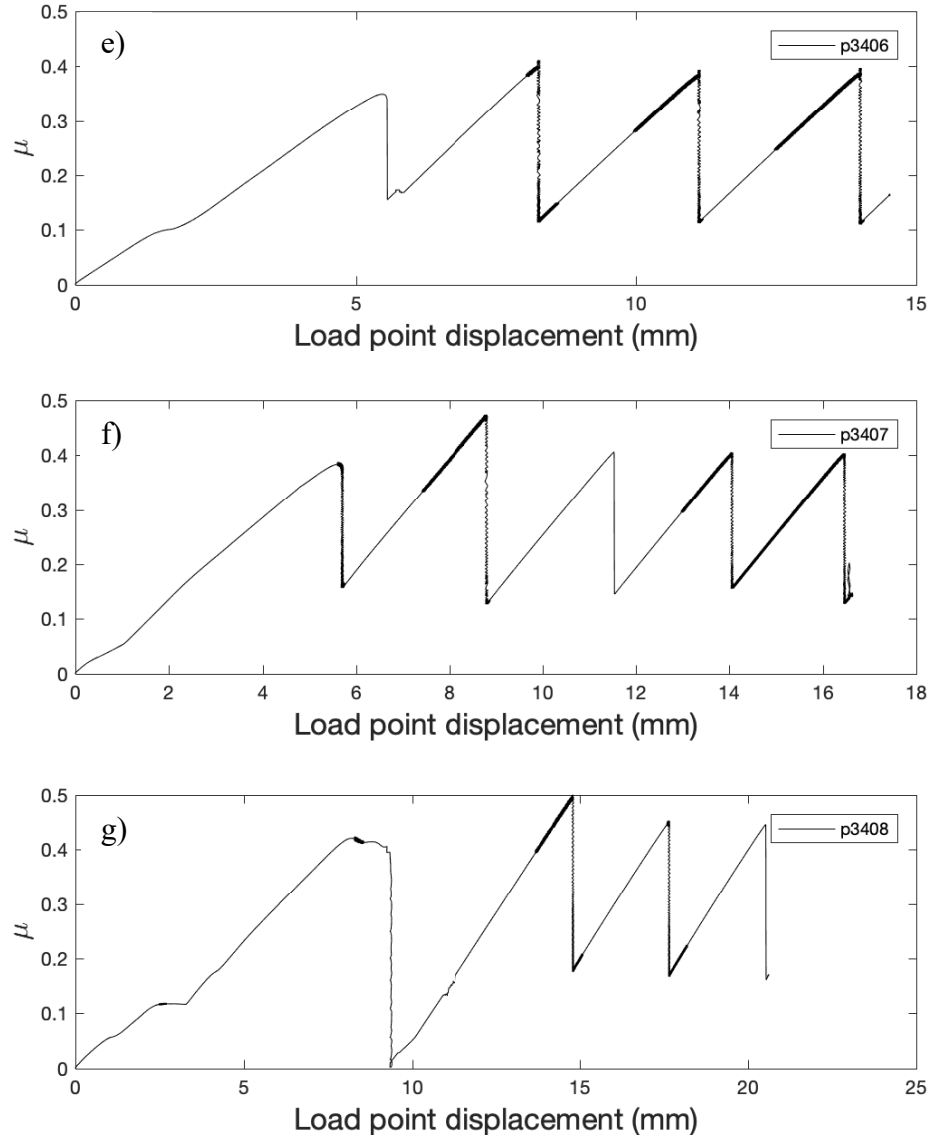

Figure S3: (a)-(g) All experiments in the study. This figures shows the friction response to increases in load point displacement for one complete experiment.

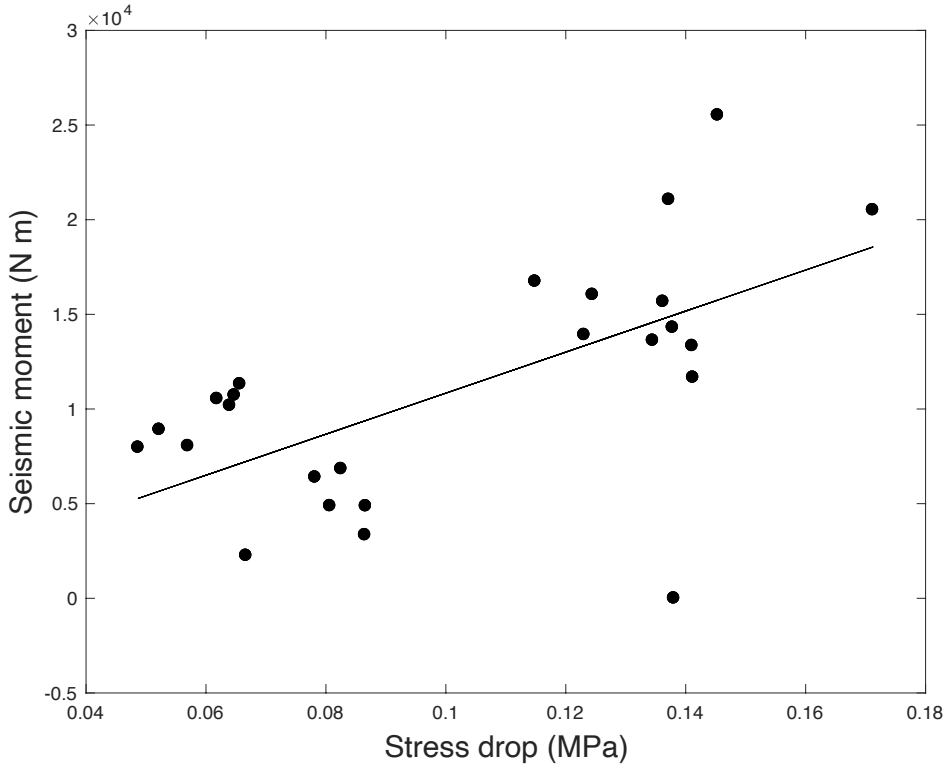

Figure S4: The relationship between stress drop and seismic moment. This seismic moment scales approximately linearly with the stress drop over the values measured in the experiments. Seismic moment, M_o, was calculated using a constant area of contact, A, and assuming a shear modulus, G, of 3 GPa and the measured displacement, d, for each slip event. The slope of the line is 0.1083 Pa (N m^{-1}).

Supporting Table 1

Experiment	Sediment amount	Velocity step μm s^{-1}	Normal stress (kPa)	Sediment type
p3347	8.7 g	10-60-100	500	Engabreen sed.
p3348	8.7 g	10-60-100	500	Engabreen sed.
p3349	20%	10-60-100	500	Engabreen basal ice sample
p3405	10.5 g	10-60	500	Engabreen sed.
p3406	5.5 g	10-60	500	Engabreen sed.
p3407	10.5 g	10-60	500	Engabreen sed.
p3408	5.5 g	10-60	500	Engabreen sed.

Experimental properties for each experiment.